COMPUTERS AND BIOMEDICAL RESEARCH 22, 405–414 (1989)

Elliptic Fourier Analysis of Cell and Nuclear Shapes

GIACOMO DIAZ, ANGELO ZUCCARELLI, ILARIA PELLIGRA, AND ALESSANDRA GHIANI

Dipartimento di Citomorfologia and Istituto di Clinica Medica, Cattedra di Genetica, Università di Cagliari, 09100 Cagliari, Italy

Received April 6, 1988

The elliptic Fourier analysis (EFA) is proposed to characterize the cell and nuclear shape. The principal feature of this method is that it decomposes shapes with a closed contour into subshapes each of which maintains a closed contour. A set of homogeneous, nonredundant descriptors, independent of the contour rotation and translation, is computed from the elliptic Fourier coefficients. These descriptors also account for the contour size and resolution. The paired analysis of the cell and nuclear shape provides an exhaustive and accurate definition of the nucleoplasmic configuration. © 1989 Academic Press, Inc.

INTRODUCTION

Cytological processes such as cell proliferation, differentiation, transformation, etc., are characterized by specific morphological changes affecting both the size and shape of cells and nuclei. Morphometric methods, while providing exhaustive information as far as concerns the size, often elude the problem of shape definition. Most of the so-called shape indices, in fact, are redundant formulations of size attributes. The "form factor," based on the area/perimeter ratio, is an emblematic case. This index is ambiguous, since the same area/perimeter ratio is shared by different "euclidean" shapes (i.e., ellipses and polygons) and, in absolute, it is also incorrect, since the perimeter length of "natural" shapes is a measure which depends largely on the resolution size (*1*).

Many biological forms, at different structural levels (organisms, organs, etc.), exhibit patterns of homologous points which configure specific anatomical shapes. For such shapes a formal statistical approach which considers the spatial arrangement of the reference points or landmarks is available (*2*). Unfortunately, points of spatial reference are lacking in cells and nuclei. Moreover, cytological observations are only partial, two-dimensional prospects of three-dimensional structures viewed through different planes of section (tissue slices) or projection (tissue appositions, smears). For these reasons, the only possible approach to the analysis of the cell and nuclear shapes is that of considering the geometric properties of the whole contour outline.

Elliptic Fourier analysis for closed contours (EFA) fits well to this purpose. The EFA algorithm is described by Kuhl and Giardina (*3*). In this paper we

0010-4809/89 $3.00

illustrate the method and its application to the analysis of the cell and nuclear shape. The graphical features of EFA should allow an intuitive understanding and evaluation of the results.

Materials and Methods

Input data are represented by point coordinates of closed contours obtained with a digitizing tablet connected to a microcomputer. Since the irregular speed of hand tracing produces an irregular point spacing, interpolation is needed in order to standardize the contour definition. For objects of comparable size, interpolation may be referred to a fixed number of equally spaced contour points. The number of 80 points was found to be adequate to reproduce most of the cell and nuclear morphological details. It may be noted that 80 points on a 40-μm perimeter are spaced by 0.5-μm intervals, a size close to the light microscope resolution.

Considering the symbology of Fig. 1 and the following definitions,

$$x_p = \sum_{j=1}^{p} Dx_j$$

$$y_p = \sum_{j=1}^{p} Dy_j$$

$$t_p = \sum_{j-1}^{p} Dt_j, \qquad T = t_k, \qquad [1]$$

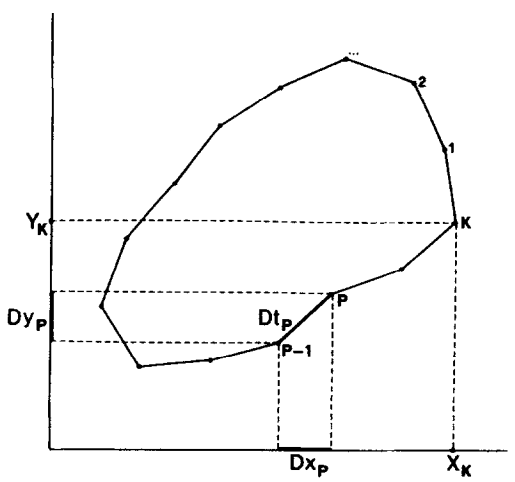

FIG. 1. Contour definition by a chain of K equally spaced point coordinates. Each chain segment between steps $p - 1$ and p has fixed length (Dt_j) and variable displacement on the x and y axis (Dx_j and Dy_j, respectively). X_k and Y_k are the coordinate pair of the last step point.

the four coefficients of the nth elliptic harmonic are obtained as

$$a_n = \frac{T}{2n^2\pi^2} \sum_{p=1}^{k} \frac{Dx_p}{Dt_p} \left[\cos \frac{2n\pi t_p}{T} - \cos \frac{2n\pi t_{p-1}}{T} \right]$$

$$b_n = \frac{T}{2n^2\pi^2} \sum_{p=1}^{k} \frac{Dx_p}{Dt_p} \left[\sin \frac{2n\pi t_p}{T} - \sin \frac{2n\pi t_{p-1}}{T} \right]$$

$$c_n = \frac{T}{2n^2\pi^2} \sum_{p=1}^{k} \frac{Dy_p}{Dt_p} \left[\cos \frac{2n\pi t_p}{T} - \cos \frac{2n\pi t_{p-1}}{T} \right]$$

$$d_n = \frac{T}{2n^2\pi^2} \sum_{p=1}^{k} \frac{Dy_p}{Dt_p} \left[\sin \frac{2n\pi t_p}{T} - \sin \frac{2n\pi t_{p-1}}{T} \right]. \qquad [2]$$

The coordinates of the original contour can be recalculated from the coefficients. For a truncated series to N harmonic, the coordinates of each contour step point p ($1 <= p <= k$) are

$$X_p = X_{\text{cen}} + \sum_{n=1}^{N} a_n \cos \frac{2n\pi t_p}{T} + b_n \sin \frac{2n\pi t_p}{T}$$

$$Y_p = Y_{\text{cen}} + \sum_{n=1}^{N} c_n \cos \frac{2n\pi t_p}{T} + d_n \sin \frac{2n\pi t_p}{T}, \qquad [3]$$

where X_{cen} and Y_{cen} are the coordinates of the harmonic centroid. X_{cen} and Y_{cen} are calculated as

$$X_{\text{cen}} = \frac{1}{T} \sum_{p=1}^{k} \left[\frac{Dx_p}{2Dt_p} (t_p^2 - t_{p-1}^2) + \left(X_k + x_{p-1} - \frac{Dx_p}{Dt_p} t_{p-1} \right) Dt_p \right]$$

$$Y_{\text{cen}} = \frac{1}{T} \sum_{p=1}^{k} \left[\frac{Dy_p}{2Dt_p} (t_p^2 - t_{p-1}^2) + \left(Y_k + y_{p-1} - \frac{Dy_p}{Dt_p} t_{p-1} \right) Dt_p \right]. \qquad [4]$$

If X_{cen} and Y_{cen} are ignored, the elliptic centroid is located on the origin (0, 0). As shown in Fig. 1, X_k and Y_k are the coordinate pair of the last step point.

The classification based on the four coefficients may be normalized with respect to the contour (a) rotation, by aligning the semimajor axis of the first harmonic on the abscissa, (b) translation, by ignoring the X_{cen} and Y_{cen} terms, and (c) size, by dividing each coefficient by the magnitude of the first semimajor axis.

Truncation of the Fourier series to N harmonics results in a shape approximation. The actual error due to this approximation may be estimated as the displacement between the original and the synthesized contour.

Each single elliptic harmonic may be geometrically visualized as a pair of orthogonal semiaxes of length

$$L_{1_n} = (a_n^{*2} + c_n^{*2})^{0.5}$$
$$L_{2_n} = (b_n^{*2} + d_n^{*2})^{0.5} \quad [5]$$

and rotation angle

$$\phi_{1_n} = \arctan (c_n^*/a_n^*)$$
$$\phi_{2_n} = \arctan (d_n^*/b_n^*), \quad [6]$$

where

$$\begin{bmatrix} a_n^* & c_n^* \\ b_n^* & d_n^* \end{bmatrix} = \begin{bmatrix} \cos \theta_n & \sin \theta_n \\ -\sin \theta_n & \cos \theta_n \end{bmatrix} \begin{bmatrix} a_n & c_n \\ b_n & d_n \end{bmatrix}, \quad [7]$$

θ being the rotation of the starting point of the harmonic

$$\theta_n = 0.5 \arctan \left[\frac{2(a_n b_n + c_n d_n)}{a_n^2 + c_n^2 - b_n^2 - d_n^2} \right]. \quad [8]$$

Of course, the semiaxes lengths L_1 and L_2 are independent of the shape rotation and translation.

Results

An example of numerical output of EFA of a neutrophil leukocyte nucleus is shown in Table 1. The graphical output of the same nucleus is drawn in Fig. 2. An effective way of comparing elliptic harmonics is that of plotting the semimajor axis versus the semiminor axis of each harmonic on the abscissa and ordinate, respectively (Fig. 3). Harmonics with the same axial ratio $AR = y/x$ will be aligned on the same line defined by the function $y = ARx$. Reference lines can be conveniently traced for different AR values. In addition, since the elliptic area is proportional to the axial product, harmonics with the same area $AP = yx$ will be aligned on the same curve defined by the hyperbolic function $y = AP/x$. Also in this case, reference curves can be traced for different AP values.

The graphical analysis may be simultaneously extended to cell and nuclear data by joining the respective plotted points with a segment (Fig. 3). The location, length, and orientation of this segment gives exhaustive information about the harmonic relationships between cell and nucleus.

Data of different leukocytes (neutrophils, lymphocytes, and monocytes) are presented in Fig. 4. The elliptic axial ratio (AR) and axial product (AP) of the first harmonic are sufficient to discriminate these types of cells. Sample statistics are reported in Table 2. In particular, as far as concerns nuclei, AR is about 0.5 in neutrophils, 0.75 in monocytes, and 0.9 in lymphocytes. AR is more stable in cells, with values ranging between 0.7 and 1. AP of neutrophil nuclei is

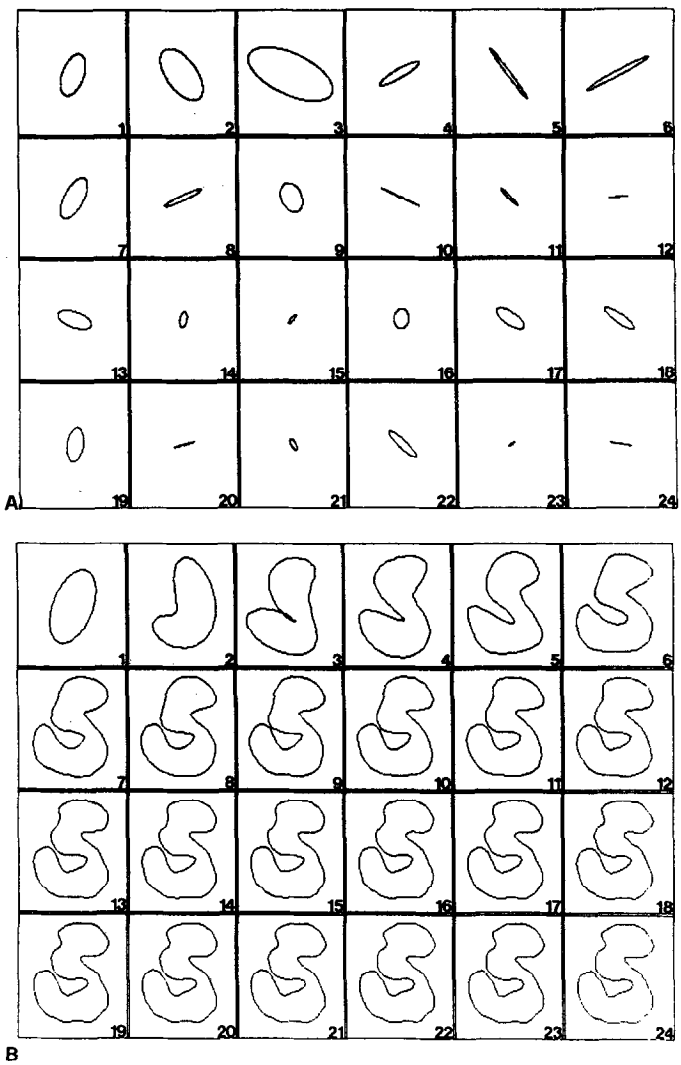

FIG. 2. Sequence of 24 elliptic harmonics of a human neutrophilic leukocyte nucleus. (A) Individual elliptic harmonics defined by the axial length and rotation. For illustrative purposes, the size of each harmonic is enlarged $n^{1.5}$ times, n being the harmonic number. The actual sizes are reported in Table 1. (B) Cumulative synthesis restoring the original shape.

small (4 to 16) as compared to that of lymphocyte and monocyte nuclei (16 to 32). In cells, except for a few small lymphocytes and large monocytes, *AP* is rather homogeneous (32 to 64).

The cumulative contribution of different harmonics to the definition of the cell and nuclear shape is shown in Fig. 5. As can be observed, a close approximation to the specific cell morphologies is reached after four harmonics.

TABLE 1

DATA OF ELLIPTIC FOURIER ANALYSIS, TRUNCATED TO 24 HARMONICS, SHOWING HARMONIC COEFFICIENTS AND DERIVED ELLIPTIC PARAMETERS (AXIS LENGTH IN MICROMETERS AND ROTATION ANGLE IN DEGREES)

	Fourier coefficients				Harmonic ellipsis axes			
					Major		Minor	
Harmonic	A	B	C	D	Length	Angle	Length	Angle
1	−7.81	−10.50	−20.01	3.80	6.14	68	3.19	338
2	−7.55	1.65	6.49	6.09	2.99	308	1.55	38
3	−6.77	−4.85	−0.16	5.03	2.55	337	1.12	67
4	1.32	2.13	1.23	0.81	0.82	29	0.16	299
5	1.59	−0.52	−1.99	0.95	0.79	307	0.05	37
6	−2.11	0.16	−1.06	0.28	0.68	27	0.05	297
7	0.26	−0.71	−0.60	−0.97	0.36	62	0.15	332
8	0.72	−0.45	0.41	−0.10	0.27	25	0.03	295
9	−0.25	0.34	0.52	0.21	0.17	292	0.11	22
10	0.48	0.33	−0.24	−0.15	0.19	334	0.00	64
11	−0.23	0.02	0.24	0.04	0.10	313	0.01	43
12	−0.09	−0.22	−0.02	−0.03	0.07	7	0.00	277
13	0.08	0.36	−0.19	−0.06	0.11	341	0.05	71
14	−0.07	0.00	−0.04	0.14	0.04	79	0.02	349
15	0.01	−0.07	0.05	−0.07	0.03	48	0.01	318
16	−0.11	0.04	0.04	0.15	0.04	83	0.03	353
17	0.15	−0.14	−0.01	0.15	0.07	326	0.03	56
18	−0.12	0.16	0.02	−0.14	0.07	325	0.02	55
19	−0.07	−0.08	0.12	−0.17	0.06	81	0.03	351
20	0.10	−0.08	0.03	−0.02	0.04	14	0.00	284
21	−0.04	0.00	0.04	0.04	0.02	300	0.01	30
22	0.13	−0.04	−0.10	0.08	0.05	316	0.01	46
23	−0.00	0.03	−0.01	0.02	0.01	35	0.00	305
24	−0.07	−0.05	0.01	0.01	0.03	352	0.00	82

Note. The graphical output of these data is shown in Fig. 2.

An intermediate result of Fourier analysis is the computation of the harmonic centroid. The displacement between the cell and the nuclear harmonic centroid provides a measure of the nucleoplasmic eccentricity.

DISCUSSION

Elliptic Fourier analysis (EFA) makes it possible to decompose closed shapes with any degree of irregularity, including edge overlapping. Shape decomposition generates subshapes each of which maintains a closed contour. These properties make EFA particularly suitable for cytological applications.

EFA shows interesting analogies with multivariate methods, in particular with Principal Components analysis which describes objects (shapes) by a set

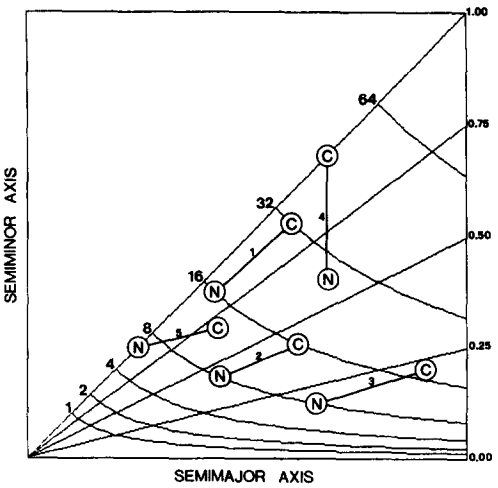

FIG. 3. Axial plot of cell (C) and nuclear (N) elliptic harmonics. The semimajor and semiminor axes of each ellipsis are plotted on the abscissa and ordinate, respectively. In addition the plot contains two sets of reference lines: straight lines, centered on the origin, which account for different elliptic shapes or axial ratios $AR = y/x$ (here traced for $AR = 1, 0.75, 0.50, 0.25$, and 0) and hyperbolic curves which account for different elliptic areas or axial products $AP = xy$ (here traced for $AP = 1, 2, 4, 8, 16, 32$, and 64). Numbers 1 to 5 illustrate five different situations. (1) The cell area ($AP = 32$) is twice that of the nucleus ($AP = 16$) while shapes are equivalent ($AR = 0.87$). (2) Cell and nucleus are smaller ($AP = 16$ and $AP = 8$, respectively) and more elliptic ($AR = 0.42$) than in the previous case 1. (3) Areas are unchanged while shapes are still more elliptic. (4) A large and circular cell ($AP = 46$, $AR = 1$) contains an elliptic nucleus ($AP = 25$, $AR = 0.54$). (5) A small and elliptic cell ($AP = 13$, $AR = 0.68$) contains a circular nucleus ($AP = 6$, $AR = 1$). Note that all the above attributes of size and shape refer to elliptic harmonics and do not apply to the actual size and shape of structures.

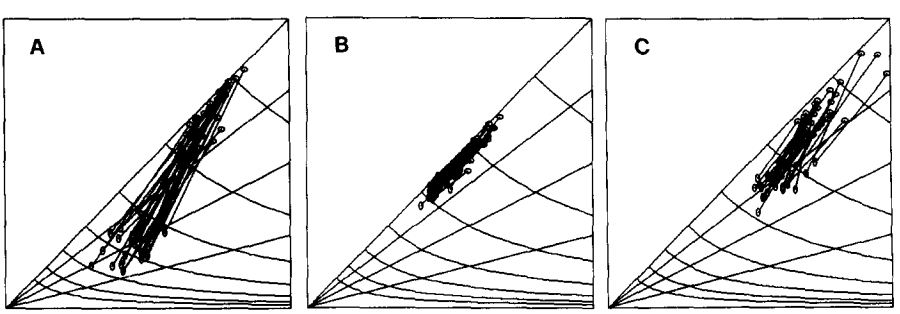

FIG. 4. Axial plots of the first elliptic harmonic of human leukocytes: neutrophils (A), lymphocytes (B), and monocytes (C). Each sample consists of 28 cells. Horizontal and vertical ovals refer to cells and nuclei, respectively. Note the characteristic harmonic pattern of each cell type.

TABLE 2

FIRST HARMONIC PARAMETERS OF THE THREE CELL SAMPLES (NEUTROPHILS, LYMPHOCYTES, AND MONOCYTES) VISUALIZED IN FIG. 4

	Neutrophils	Lymphocytes	Monocytes
Cell			
Semimajor axis	6.23 ± 0.50	4.91 ± 0.49	6.57 ± 0.69
Semiminor axis	5.79 ± 0.73	4.67 ± 0.49	5.89 ± 0.67
Nucleus			
Semimajor axis	3.85 ± 0.54	4.01 ± 0.31	5.12 ± 0.45
Semiminor axis	1.85 ± 0.46	3.67 ± 0.25	3.76 ± 0.37

Note. Data are expressed in micrometers (mean ± standard deviation). For each sample $n = 28$.

of mutually independent, homogeneously scaled, and hierarchically ordered new variables (harmonics). Indeed, multivariate statistics applied to dimensional morphometric data (*4, 5*) are often concerned with the recognition of shape attributes.

The approximation of the Fourier-synthesized shape to the original shape depends on the number of harmonics considered. On the other hand, the number of representative harmonics has a limit in the resolution of the original contour. A practical consequence of this fact is that the same cell observed at the light and electron microscope will give comparable results only in the first group of harmonics which account for the common lower (light microscope) resolution.

The length of the elliptic semiaxis is independent of both translation and rotation. However, it may be useful to consider the location and orientation of elliptic harmonics in order to identify possible structural relationships in terms of nucleoplasmic eccentricity and anisotropy.

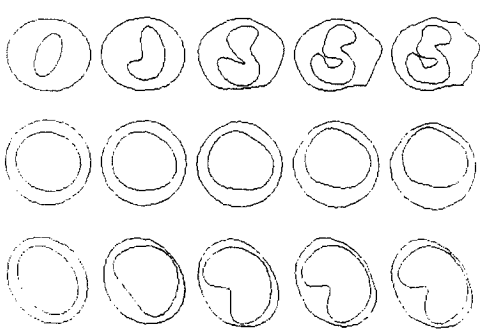

FIG. 5. Cumulative cell and nuclear shape synthesis obtained with 1, 2, 4, 8, and 12 harmonics (from left to right) of a single neutrophil (up), lymphocyte (mid), and monocyte (down).

If one excepts some extreme situations where the nucleus is compressed at one cell pole by cumulating cytoplasmic inclusions, as in the case of fat cells and mucous secreting cells, the nuclear shape is a structurally independent character. This is demonstrated by the stability of the nuclear shape after nuclear isolation (*6*) and during nuclear rotation in living cells (*7*).

It is interesting to note that even neutrophil nuclei display quite homogeneous data. This suggests that the apparent irregularity of these polymorphic nuclei may be referred to simple structural factors. This is indirectly supported by some correspondences between the sequence of cell shapes decomposed by EFA and the sequences of shapes shown by the same cell during its maturation (for early leukocytic stages see, for example, Bessis (*8*)). This fact, which points to the problem of the model of cell morphogenesis, may not be a mere coincidence. Since the cell at the end of mitosis exhibits a nearly round (spherical) cytoplasm and nucleus, subsequent shape changes may be conceived as the effect of elliptic deformations.

The parallel analysis of the cell and nuclear shape provides a complete definition of the cell morphology. As our findings show, neutrophils, lymphocytes, and monocytes can be distinguished on the basis of just one (the first) harmonic (Fig. 5). Obviously, concrete problems of discrimination could require the evaluation of a higher number of harmonics, adequate to represent less evident morphological differences. For example, normal blood lymphocytes and peripheral CLL (chronic lymphocytic leukemia) cells, which display equivalent dimensional distributions (*9*), may be separated on the basis of shape differences recognizable in the first 12 harmonics (unpublished data).

The quantitative relationship between cell and nuclear shape may be globally indicated as nucleoplasmic "shape" ratio in analogy with the classic nucleoplasmic "volume" ratio. Relevant biological implications of this shape ratio may be found in the specific cytoskeletal organization, motility, adhesion to substrate, etc., of different cell types.

ACKNOWLEDGMENTS

This research was supported by grants from M.P.I. and C.N.R., Roma, Italy.

REFERENCES

1. MANDELBROT, B. B. "The Fractal Geometry of Nature." Freeman, New York, 1977.
2. BOOKSTEIN, F. L. A statistical method for biological shape comparisons. *J. Theor. Biol.* **107,** 475 (1984).
3. KUHL, F. P., AND GIARDINA, C. R. Elliptic Fourier features of a closed contour. *Comp. Graph. Image Proc.* **18,** 236 (1982).
4. OLSON, A. C., LARSON, N. M., AND HECKMAN, C. A. Classification of cultured mammalian cells by shape analysis and pattern recognition. *Proc. Natl. Acad. Sci. USA* **77,** 1516 (1980).
5. REYMENT, R. A., BLACKITH, R. E., AND CAMPBELL, N. A. "Multivariate Morphometrics." Academic Press, London, 1984.

6. AARONSON, R. P., AND BLOBEL, G. Isolation of nuclear pore complexes in association with a lamina. *Proc. Natl. Acad. Sci. USA* **72,** 1007 (1975).
7. BARD, F., BOURGEOIS, C. A., COSTAGLIOLA, D., AND BOUTEILLE, M. Rotation of the cell nucleus in living cells: A quantitative analysis. *Biol. Cell* **54,** 135 (1985).
8. BESSIS, M. "Cellules du Sang Normal et Pathologique." Masson, Paris, 1972.
9. JUAN, J., SIGAUX, F., AND FLANDRIN, G. Automated classification of lymphoid cells. *Anal. Quant. Cytol. Histol.* **7,** 38 (1985).